

# Tolerancing and corner cases in optical simulation

Robert P. Dahlgren\* and Kenneth D. Pedrotti  
Baskin School of Engineering, UC Santa Cruz  
1156 High Street, Santa Cruz, CA 95064-1077 USA

## ABSTRACT

Our work discusses the tolerance modeling of an optical fiber that is inserted into a cylindrical alignment bore. We note that some commercial optical simulation software suites have the mechanical tolerance operands entered in Cartesian coordinates and if radial variation is entered as simple X and Y de-centering, there arises a kind of "corner condition" where fiber in the opto-mechanical model is offset more than is possible in the physical implementation resulting in an overly-conservative estimate of the worst-case coupling efficiency. Approaches to avoid this over estimation are presented and discussed.

**Keywords:** Modeling and simulation, optical data interconnect, fiber-optic modules, optics

## 1. INTRODUCTION

Polymer optical fiber (POF) links are under investigation for multi-gigabit-class data communication, over transmission distance of several centimeters to many meters<sup>1</sup>. Two key components in an optical fiber data link are a transmitter optical subassembly (TOSA) and receiver optical subassembly (ROSA). The ROSA contains a receptacle for the POF, light collection optics, and a high-speed photodetector to perform optical-to-electrical conversion. The TOSA employs an optical source such as a laser diode to launch amplitude-modulated light into the fiber waveguide as shown in Figure 1, and may include "conditioned launch" features<sup>2</sup>. To enable multi-gigabit operation, electrical I/O is often performed via controlled impedance transmission lines, using electrical connections that attempt to minimally perturb the signal at ultra-high frequencies.

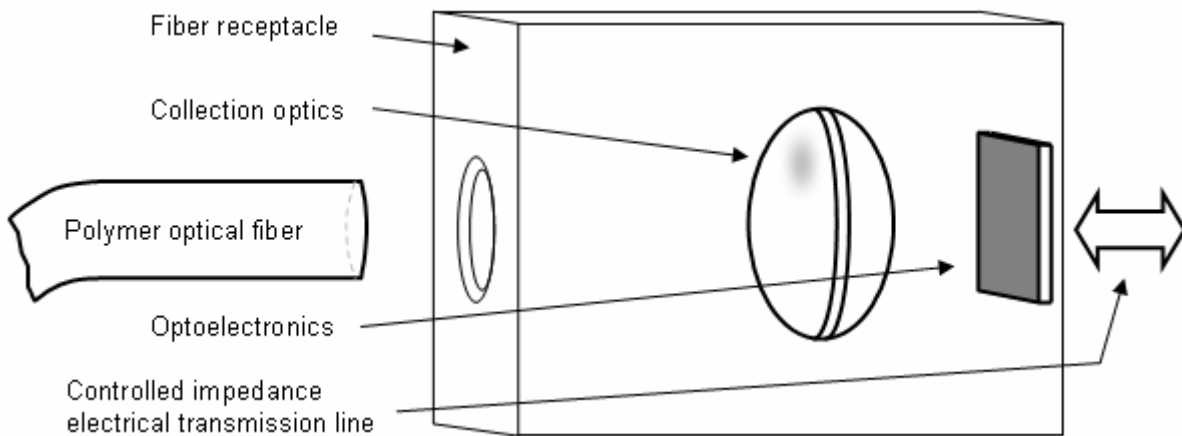


Figure 1. Block diagram of TOSA or ROSA showing major components, and uninstalled POF. Receptacle bore and fiber retention mechanism is not shown for clarity. In the drawing light would propagate from fiber-to-detector for a ROSA, and right-to-left for a TOSA.

\* rdahlgren@soe.ucsc.edu; phone +1.831.459.4283

POF has an extremely low cost of installation because it does not require polishing, making the TOSA and ROSA assemblies an increasing portion of the total link cost. To realize truly low costs in a hypothetical mass production situation places further constraints on the design. Moreover, it is demanded that active optical alignment be avoided, and standard electronics mass production process be used (e.g. die attach, pick-and-place, and wirebonding). With this in mind we chose chip-on-board (COB) assembly techniques for prototype assembly, with an eye toward chip-scale packaging (CSP) in the long run<sup>3</sup>.

### 1.1 Description

Figure 2 is a cross-section of the cylindrical fiber insertion bore in the receptacle, typically made from an injection molded amorphous polymer such as PEI (polyetherimide), which has reasonable transmission at 850 nm. The fiber bore is a precision-molded feature, which has dimensional tolerances  $\sim 5 \mu\text{m}$ . Also shown are other features such as a beveled lead-in area to ease fiber installation, and a small ledge to limit the POF longitudinal insertion. Beyond the edge of the primary bore is a smaller-diameter counterbore, which serves as an air gap for free space propagation, protects the fiber core from physical contact, and fixes the gap between the fiber and the vertex of the collection optics.

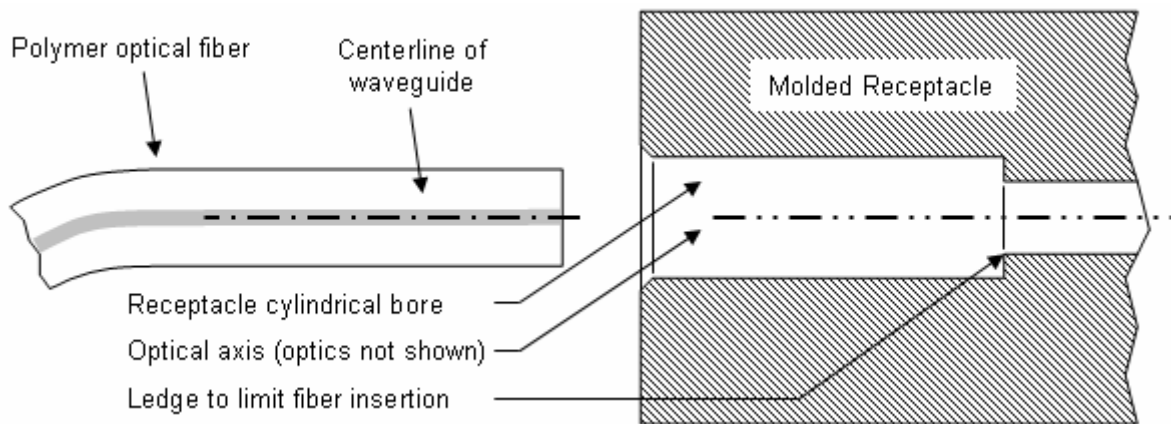


Figure 2. Cross-sectional side view of the optical fiber receptacle showing the two cylindrical counterbores used to mechanically align the fiber waveguide with respect to the collection optics (not shown).

Likewise, the POF itself is a precision structure with diametral and concentricity tolerances  $< 10 \mu\text{m}$ . For clarity the fiber retention mechanism is not shown in this cross-section, nor is the collection optics.

### 1.2 Ferrules

For a number of reasons it was chosen to avoid the use fiber ferrules for this application:

- The envisioned application has only a few mate-demate cycles.
- POF is available with a large outside diameter and high Young's modulus.
- The optical waveguide has tightly-controlled concentricity to the POF outside diameter.
- Avoid the problem of secondary alignment and all of the associated dimensional uncertainties.
- Avoids the summing of additional fitment gaps in the tolerance budget.
- Allows for a smaller overall assembly.

## 2. METHODOLOGY

When modeling a design with optical simulation software, to permit independent alignment of two optical subsystems (waveguide and collection optics), a coordinate break is preferable to surface/group decenters and tilts. The relationship between the optical axis of the waveguide and the optical axis of the collection optics is illustrated in Figure 3, which also shows the coordinate transformation for 5 out of 6 degrees of freedom. Because of the cylindrical symmetry of the

optical design, the system is independent of rotation about the Z-axis. The 6<sup>th</sup> degree of freedom, changes in the Z-dimension along an optical axis, is handled by a separate operation.

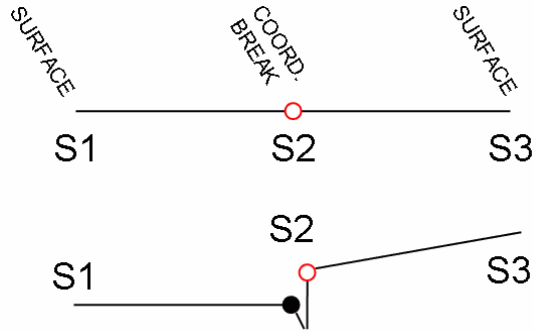


Figure 3. Coordinate break (red circle) between optical axes, before and after transformation: First decenter X, then decenter Y, then tilt about the X-axis, tilt about the Y-axis, and finally, tilt about the Z-axis.

After an initial layout of the optical system is performed using commercial optical design software, the design is optimized through application of constrained, damped least-square (DLS) routines<sup>4</sup>. Subsequently, a global optimization is performed, through use of a genetic optimization technique<sup>5</sup> to ensure that a true optimum has been found. Finally, sensitivity to mechanical misalignment is estimated with the Monte Carlo method, based on the relevant mechanical and optical degrees of freedom having finite tolerances. When running the Monte Carlo analysis, it is very important to provide the correct tolerance range, as this determines over which range the values will be selected about the nominal. The methodology to correctly sum the mechanical uncertainties is now discussed, assuming the centroids of the cylindrical objects are coincident with that of the ideal shape under discussion.

We will use the following convention: Uppercase variables are used for nominal values and lowercase variables are the tolerance range, as shown below.

$$D_{\text{clad}} - d_{\text{clad}} < \text{possible diameter} < D_{\text{clad}} + d_{\text{clad}} \quad (1)$$

For the case of symmetrical error bounds, a 750 micron diameter fiber with a diameter tolerance of  $\pm 5$  microns results in

$$D_{\text{clad}} = 750 \mu\text{m} \quad \text{and} \quad d_{\text{clad}} = 5 \mu\text{m}$$

It will also be useful to sometimes use non negative radial values, to permit the straightforward summing with concentricity errors. This may be written as

$$D_{\text{clad}} \pm d_{\text{clad}} = 2(R_{\text{clad}} \pm r_{\text{clad}}) \Rightarrow R_{\text{clad}} = D_{\text{clad}}/2 \quad \text{and} \quad r_{\text{clad}} = d_{\text{clad}}/2 \quad (2)$$

$$R_{\text{clad}} = 375 \mu\text{m} \quad \text{and} \quad r_{\text{clad}} = 2.5 \mu\text{m}$$

Concentricity of the j<sup>th</sup> to the k<sup>th</sup> element is radial by definition, and is represented by a lowercase variable having subscripts j and k.

## 2.1 Nominal Dimension Design

To derive the target bore design given the fiber dimensions, the following approach is used for non press-fit applications, where it is desired to have a mechanical slip-fit and avoid binding between the fiber and the bore under all conditions. An industry rule of thumb for fiber-in-connector is a proportionality constant  $\gamma$  of 0.5% of the nominal diameter for hard materials such as ceramic and metal, and 1% for softer materials<sup>6</sup>. For maximum fiber size and worst-case (minimum) bore diameter, this condition is met if

$$D_{\text{bore}} - d_{\text{bore}} > D_{\text{clad}} + d_{\text{clad}} + \gamma D_{\text{clad}} \quad \text{where} \quad \gamma = 0.01 \quad (3)$$

To minimize misalignment the bore diameter should be as small as possible yet still met our constraint, therefore we can replace the inequality with an identity, and next solve for the design bore diameter, and nominal gap size:

$$D_{\text{bore}} = D_{\text{clad}} + d_{\text{clad}} + \gamma D_{\text{clad}} + d_{\text{bore}} \quad (4)$$

$$\text{Nominal gap} = D_{\text{bore}} - D_{\text{clad}} = d_{\text{clad}} + \gamma D_{\text{clad}} + d_{\text{bore}} \quad (5)$$

$$\text{Maximum gap} = D_{\text{bore}} + d_{\text{bore}} - (D_{\text{clad}} - d_{\text{clad}}) = 2 d_{\text{clad}} + \gamma D_{\text{clad}} + 2 d_{\text{bore}} \quad (6)$$

$$\text{Minimum gap} = \gamma D_{\text{clad}} \quad (7)$$

The design value of  $\gamma D_{\text{clad}}$  in our example is chosen to be 6  $\mu\text{m}$ . Parameters provided by the POF vendor and molding supplier are listed in the 2nd column in Table 1 and are used to compute the nominal bore diameter  $D_{\text{bore}}$  and gap sizes which are summarized in the right column, converting to millimeters.

Table 1. Design table for TOSA/ROSA receptacle bore inside diameter.

POF vendor "C" specifications	$\mu\text{m}$		Variable	mm
Nominal fiber O.D.	750		$D_{\text{clad}}$	0.750
Fiber O.D. Tolerance	$\pm 5$		$d_{\text{clad}}$	0.005
Fiber-bore Fitment $\sim 1\%$	6		$\gamma D_{\text{clad}}$	0.006
Molding Tolerance $6\sigma$	$\pm 5$		$d_{\text{bore}}$	0.005
Nominal Bore I.D.	Eq. (4)	$\Rightarrow$	$D_{\text{bore}}$	0.766
Nominal Gap	Eq. (5)			0.016
Maximum Gap	Eq. (6)			0.026

For industry standard fiber optic connectors, nominal dimensions along with mechanical tolerances for most fiber interfaces are codified in fiber connector intermatability standards.

## 2.1 Waveguide-to-optics decentering tolerance

Table 2 repeats some of the above parameters, only the radial uncertainties are added together in the right-hand column, also converting from microns to millimeters. In this manner the net effect of gaps, size error, and concentricity may be calculated. Note that the worst-case value (less the core-clad concentricity) is equal to half of Eq. (6).

Table 2. Tolerance table for TOSA/ROSA receptacle for decentering uncertainty.

POF vendor "C" specifications	$\mu\text{m}$		Variable	mm
Nominal core diameter	120		$R_{\text{core}} = 0.060$	
Core diameter tolerance	$\pm 10$		$r_{\text{core}} = 0.005$	[7]
Nominal fiber O.D.	750		$R_{\text{clad}} = 0.375$	
Fiber O.D. Tolerance	$\pm 5$		$r_{\text{clad}}$	0.0025
Core-clad Concentricity	$\leq 5$		$c_{\text{cc}}$	0.005
Molding Tolerance $6\sigma$	$\pm 5$		$r_{\text{bore}}$	0.0025
Clad-bore Concentricity	$\frac{1}{2}$ Eq. (5)		$c_{\text{gap}}$	0.008
Worst-case summation		TUDX TUDY	$\sum_{ijk} r_i + c_{jk}$	$\pm 0.018$
Root-sum-square		TUDX TUDY	$\sqrt{\sum r_i^2 + c_{jk}^2}$	$\pm 0.010$

The bottom line value will be used for inputs to the tolerance spreadsheet in the Monte Carlo simulator for two of the six degrees of freedom for decentering, namely tolerance on coordinate break decentering in X (TUDX) and decentering in Y (TUDY) operands. The worst-case summation is the most conservative way to tally the tolerances; and the RSS

value may be used if all of the uncertainties are statistically independent. In general, the parameters are statistically independent, but not all of them. For example the error in fiber core diameter and the fiber cladding diameter may be related because of the way that POF is manufactured. However, it is common practice in the electronics industry to consider all of the variables to be independent, and RSS methodology may be used<sup>8</sup>, so we are confident to use the value of  $\pm 10 \mu\text{m}$  for our  $6\sigma$  decentering value.

### 2.2 Waveguide-to-optics longitudinal tolerance

We now examine the positional uncertainty of the fiber in the receptacle along the z-axis. The ledge which limits fiber insertion depth has a finite tolerance with respect to its ideal position, due to the molding process. For additional reasons the waveguide may fall short from the ledge, which makes for asymmetric tolerance bounds for this degree of freedom. For this analysis the uncertainty is made symmetric by adjusting the nominal insertion position slightly outwards.

Table 3. Tolerance table for TOSA/ROSA receptacle for longitudinal uncertainty.

Design specifications	$\mu\text{m}$		Variable	mm
Nominal fiber insertion	$L_{\text{bore}} = 1000$			
Minimum insertion margin	0			
Maximum insertion margin	25		$Z_{\text{fiber}}$	0.0125
Maximum cleave angle	$\pm 2^\circ$			
Minimum shift due to cleave	0			
Maximum shift due to cleave	13.1		$Z_{\text{cleave}}$	0.0065
Molding Tolerance $6\sigma$	$\pm 5$	$\Rightarrow$	$Z_{\text{bore}}$	0.005
Worst-case summation		TTHI	$\sum_{ijk} r_i + c_{jk}$	$\pm 0.024$
Root-sum-square		TTHI	$\sqrt{\sum r_i^2 + c_{jk}^2}$	$\pm 0.015$

Both worst-case and RSS values are shown. The  $6\sigma$  result from Table 3 is plugged into the tolerance on thickness (TTHI) operand of the Monte Carlo simulator. Care must be taken to ensure that automatic compensators are not turned on for this operand, which would erroneously adjust the optical path length.

### 2.3 Waveguide-to-optics tilt tolerance

This is the non-parallelism of the waveguide optical axis to the collection optics. There are two main contributors: the POF tilting in the oversized bore, and beam deviation due to non-perpendicular endface of the POF. The first term is derived from Figure 4(a) using trigonometry and equation (8) assuming the fiber and bore are rigid bodies.

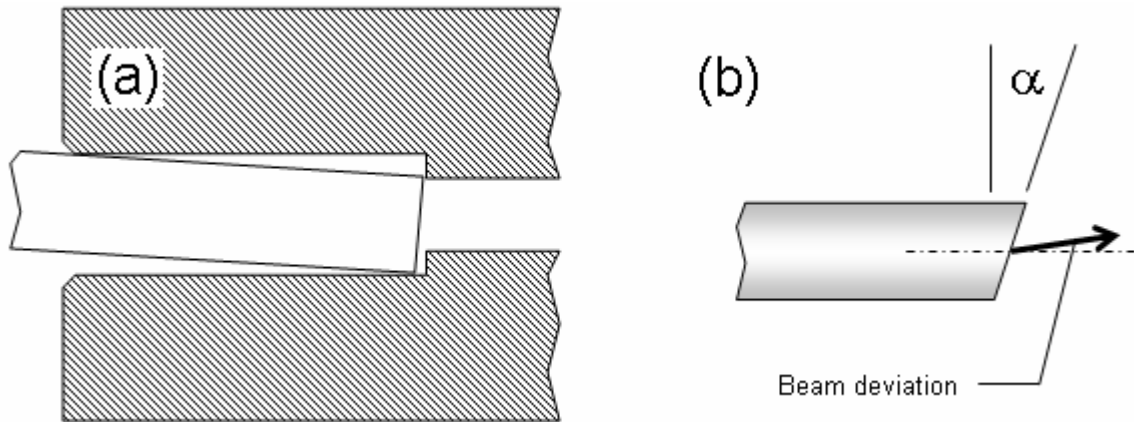


Figure 4 (a) illustration of fiber tilting in bore (b) effect of refraction with non-perpendicular POF endface.

and does not include effects of deformation due to side-loading of the POF. The nominal angle is zero and the angular uncertainty is derived from the worst-case gap value (Eq. 6) and the bore depth

$$\Phi = 0 \quad \text{and} \quad \phi = \arctan [(2 d_{\text{clad}} + \gamma D_{\text{clad}} + 2 d_{\text{bore}}) / L_{\text{bore}}] \quad (8)$$

Now refer to Figure 4(b), which illustrates the cleave-induced beam tilt<sup>9</sup>. This is found to first order by applying Snell's law in the limit of small angles resulting in

$$\Phi = 0 \quad \text{and} \quad \phi \approx (n-1) |\alpha| \quad (9)$$

POF may be routinely cut with perpendicularity <math>\pm 2^\circ</math>. Given the worst-case cleave angle  $\alpha = 2^\circ$  and fiber refractive index is  $n = 1.35$  yields an uncertainty limited to of  $0.70^\circ$  due to imperfect cleaving. The bore draft angle was specified to be zero, for this low aspect-ratio bore design.

Table 4. Tolerance table for TOSA/ROSA receptacle for angular uncertainty.

Design specifications	degrees		Variable	degrees
Maximum tip angle	Eq. (2)	⇒	$\phi_b$	1.5
Maximum angle due to cleave	Eq. (3)		$\phi_c$	0.7
Draft angle	$2 \sim 3^\circ$		$\phi_d$	0.0
Worst-case summation		TUTX TUTY	$\sum_{ijk} r_i + c_{jk}$	$\pm 2.2$
Root-sum-square		TUTX TUTY	$\sqrt{\sum r_i^2 + c_{jk}^2}$	$\pm 1.65$

The RSS sum derived from the  $6\sigma$  data is entered into the tolerance of tilt about X operand (TUTX) and TUTY operands, which are the 3rd and 4th degrees of freedom.

### 2.4 Waveguide-to-optics rotation tolerance

Because of cylindrical symmetry, and the neglecting of polarization effects, we may ignore the 5th degree of freedom (in this case TUTZ) in the tolerance budget.

## 3. RESULTS

### 3.1 Monte Carlo Simulation

The tolerance data editor was populated as described, and when the Monte Carlo simulator was invoked on our optical design<sup>10</sup>, one hundred full field spot diagrams at the image plane were overlaid, shown in Figure 5.

Note that the image is decidedly not circularly symmetric, even though the optical design is rotationally symmetric with respect to the optical axis.

### 3.2 Discussion

After some research it was noted that some commercial optical simulation software suites have the mechanical tolerance operands entered in Cartesian coordinates, i.e. displacement is represented in X, Y and Z coordinates, and tilts are about X, Y, and Z axes.

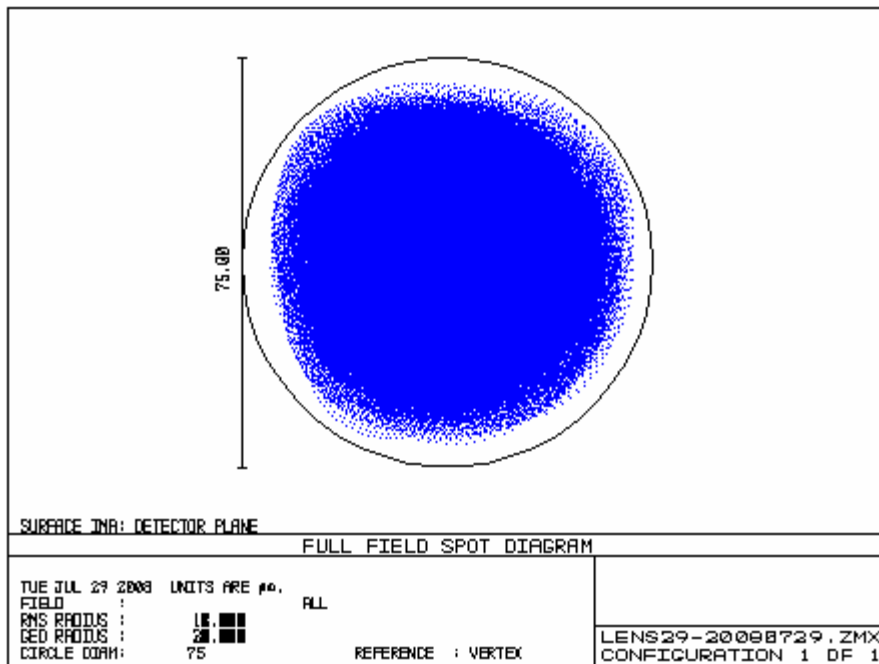


Figure 5. Geometric full field spot diagram for 100 Monte Carlo runs. Note the non circular shape.

For the case of optical fiber in a cylindrical bore, if radial variation is entered as X and Y decentering there arises a kind of "corner condition" where fiber in the opto-mechanical model is offset more than is possible in the physical implementation. Figure 6 illustrates this situation. A similar situation occurs for the tilting of the fiber bore about the Cartesian X and Y axes, which also contributes to the non symmetric result. This could result in the underestimation of the system misalignment margins.

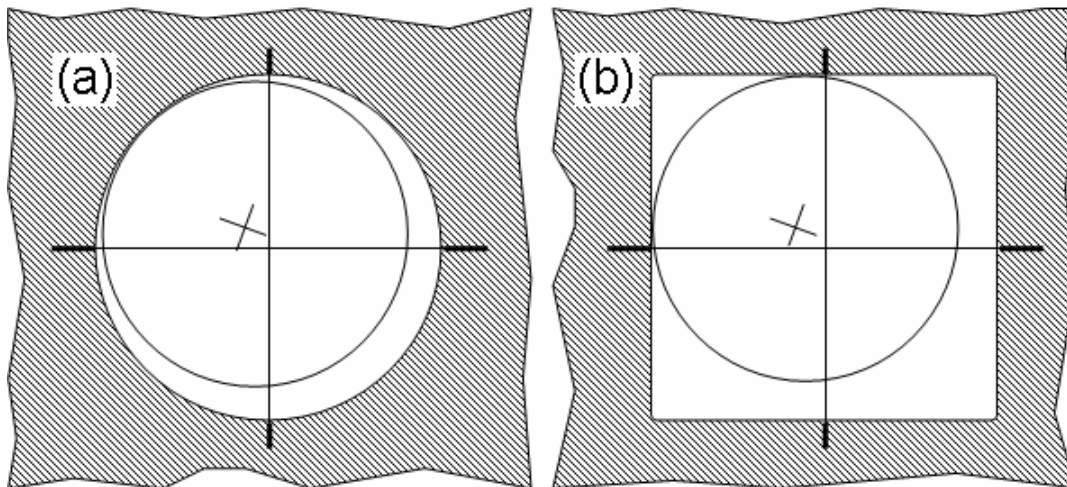


Figure 6. Actual (a) and simulated (b) model of fiber in bore showing overestimation of decentering value.

### 3.3 Proposed Solution

To achieve the correct results, a slightly modified optical layout illustrated in Figure 7 is proposed, along with a slightly modified Monte Carlo simulation. In the new optical layout, a 2nd coordinate break S3 is placed at a zero distance from

the first coordinate break, and the first coordinate break S2 is now used just for decentering along one axis only. The second coordinate break S3 is reserved for tilting. After each transformation, the rotation about the Z-axis is completely unconstrained, in effect making the transformation from rectangular to polar coordinates if a large enough number of Monte Carlo runs are performed.

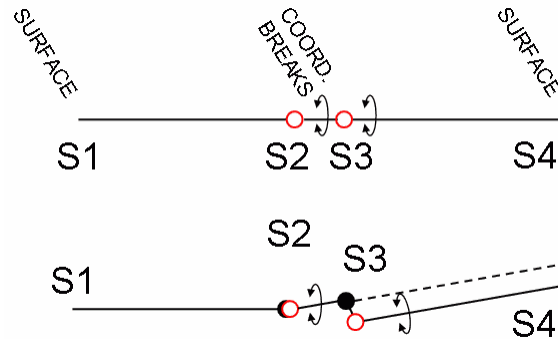


Figure 7. Improved dual coordinate break in optical axis, before and after: First decenter X only, then rotate  $\pm 180^\circ$  about the Z axis. A second coordinate break at zero distance then tilts about the Y axis only, followed by another  $\pm 180^\circ$  about Z.

Table 5. Tolerance Data Editor operands for Monte Carlo simulation. Decentering units are mm, and tilt is in degrees.

Original Method (Figure 3)				Proposed Method (Figure 7)			
Operand	Surf	Min	Max	Operand	Surf	Min	Max
TUDX	2	-0.010	+0.010	TUDX	2	-0.010	+0.010
TUDY	2	-0.010	+0.010	TUTZ	2	-180	+180
TUTX	2	-1.65	+1.65	TUTY	3	-1.65	+1.65
TUTY	2	-1.65	+1.65	TUTZ	3	-180	+180

The modified Monte Carlo inputs are listed in Table 5. By using only one Cartesian coordinate, and spinning around the Z-axis, the model correctly simulates the misalignments, yielding a symmetric result as shown in Figure 8.

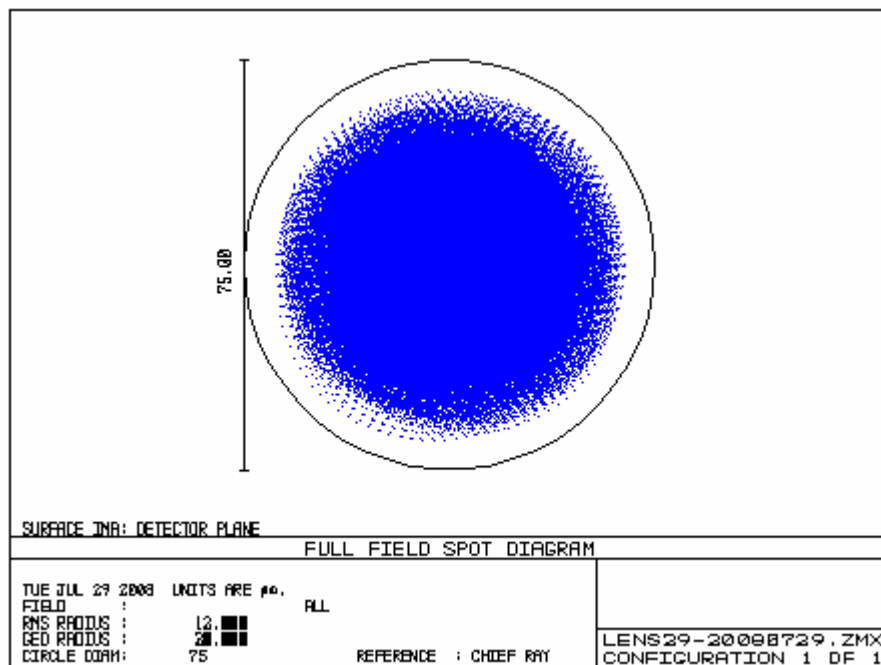


Figure 8. Geometric full field spot diagram for 100 Monte Carlo runs.

## 4. CONCLUSIONS

For an example of fiber-to-detector coupling efficiency, this “corner case” can result in an overly-conservative estimate of the worst-case coupling efficiency, because the Monte Carlo algorithm will select fiber alignment values that are unrealistically large in some of the Monte Carlo runs. The result is that computed figures of merit such as worst-case coupling efficiency will be erroneous, and any statistical analysis based upon the Monte Carlo runs will thus be skewed.

Simple tolerance reduction through application of a geometric factor, say 0.707, will return incorrect results, as will an artificial constraint of decentering along only one axis during simulation. However, a properly modified simulation can establish the correct bounds for a worst-case coupling efficiency error estimate. This is performed in large part by unconstraining tilt about the optical axis in the Monte Carlo simulation.

## ACKNOWLEDGEMENT

The authors would like to acknowledge the support of Avago Technologies and FiberFin Corporation. We would also like to thank the Astronomy Department and the Institute of Particle Physics at the University of California, Santa Cruz.

## REFERENCES

- [1] Ziemann, O. and White, W., “100 Mbit/s - Gbit/s - 10 Gbit/s and beyond, the use of POF in home networking and interconnection,” Proc. ECOC, 2007.
- [2] Raddatz, L., White, I., Cunningham, D. and Nowell, M., “An experimental and theoretical study of the offset launch technique for the enhancement of the bandwidth of multimode fiber links,” IEEE JLWT 16(3), 324 (1998).
- [3] For example Avago Technologies HSDL-3208 optical IRDA interface.
- [4] Geary, J. M., [Introduction to Lens Design], Willmann-Bell Publishers, (2002).
- [5] Moore, K. E., "Algorithm for global optimization of optical systems based upon genetic competition," Proc. SPIE 3780, 40-47 (1999).
- [6] Mulligan, P., personal communications (2006).
- [7] The tolerance on the core size and NA are not tallied here but its effect is modeled elsewhere in the simulation.
- [8] Mohan, J., personal communications (2008).
- [9] Gao, C. and Farrell, G., “Numerical aperture characteristics of angle-ended plastic-optical fiber,” Proc. SPIE 4876, 404 (2003).
- [10] Dahlgren, R., Wysocki, J. and Pedrotti, K., “Non-imaging optical concentrators for low-cost optical interconnect,” Proc. SPIE 7059, (San Diego, 2008).